ARCHIVES OF ACOUSTICS
36, 4, 913–926 (2011)

DOI: 10.2478/v10168-011-0061-5

Golay Coded Sequences in Synthetic Aperture Imaging Systems

Ihor TROTS, Yuriy TASINKEVYCH, Andrzej NOWICKI, Marcin LEWANDOWSKI

Department of Ultrasound
Institute of Fundamental Technological Research
Polish Academy of Sciences
Pawińskiego 5B, 02-106 Warszawa, Poland
e-mail: igortr@ippt.gov.pl

(*received October 5, 2011; accepted November 29, 2011*)

The paper presents the theoretical and experimental study of synthetic transmit aperture (STA) method combined with Golay coded transmission for medical ultrasound imaging applications. The transmission of long waveforms characterized by a particular autocorrelation function allows to increase the total energy of the transmitted signal without increasing the peak pressure. It can also improve signal-to-noise ratio and increase the visualization depth maintaining the ultrasound image resolution.

In the work the 128-element linear transducer array with 0.3 mm pitch excited by the 8 and 16-bits Golay coded sequences as well as a one cycle at nominal frequencies 4 MHz were used. The comparison of 2D ultrasound images of the tissue mimicking phantoms is presented to demonstrate the benefits of coded transmission. The image reconstruction was performed using synthetic STA algorithm with transmit and receive signals correction based on a single element directivity function.

Keywords: ultrasound imaging, synthetic aperture, beamforming, radiation pattern, coded sequences, Golay codes.

1. Introduction

Ultrasound imaging has become one of the primary techniques for medical imaging mainly due to its accessibility, non-ionizing radiation, and real-time display. In ultrasonography the most commonly used image quality measures are spatial resolution and image contrast resolution which can be determined in terms of beam characteristics of an imaging system: beam width and side-lobe level. High resolution ultrasound images can be obtained by using array transducers and advanced beam-forming techniques applying synthetic aperture

(SA) imaging method. The basic idea of the SA method is to combine information from emissions close to each other. This method is a contrast to the conventional beamforming, where only one image line is created during a transmission.

Another crucial factor for image quality in ultrasound imaging is decreasing of the signal-to-noise ratio (SNR) with depth. The severe attenuation of the ultrasonic signals in the tissue results in echoes from large depths literally buried in noise. To overcome this problem, the long wide band transmitting sequences and compression techniques on the receiver side can be applied. The average transmitted energy increases proportionally to the length of the code. There are several papers in literature concerning similar boundary-condition problem of signal compression in medical diagnostic imaging (Nowicki *et al.*, 2003; Klimonda *et al.*, 2005).

Till now, in SA methods it is assumed that the transmit and receive elements are the point-like sources and the dynamical focusing is realized by finding the geometric distance from the transmitting element to the imaging point and back to the receiving element. But when the element size is comparable to the wavelength the influence of the element directivity on the wave field generation and reception become significant and if ignored might be a source of errors and noise artefacts in the resulting image. In this paper the STA algorithm, which takes into account the single element directivity to improve the quality of the resulting image, is investigated. For this purpose the array element is modeled as a narrow strip transducer with a time harmonic uniform pressure distribution over its width for the far-field radiation pattern calculation. An analytical expression for the corresponding directivity function is available in literature by use of the proper interpretation of the Rayleigh-Sommerfeld theory (Selfridge *et al.*, 1980) resulting in multiplication the acoustic pressure value by an extra $\cos(\theta)$ term. The far-field assumption is shown to be acceptable in the considered cases of the transducer dimension to wavelength ratios. As a result the comparison of computer simulation images of the wire phantom obtained for one short cycle and Golay complementary sequences used *Field II* simulation program (Jensen, 1996) for Matlab environment are presented. The applied coded sequences increased the visualization depth maintaining high image resolution.

2. Synthetic transmit aperture method

As an alternate to the conventional phased array imaging technique the synthetic transmit aperture (STA) method can be used (Hongxia, 1997; Trahey, Nock, 1992; Trots *et al.*, 2009; Trots *et al.*, 2010). It provides the full dynamic focusing, both in transmit and receive modes, yielding the highest imaging quality. In the STA method at each time one array element transmits a pulse and all elements receive the echo signals, where data are acquired simultaneously from all directions over a number of emissions, and the full image can be recon-

structed from these data. The advantage of this approach is that a full dynamic focusing can be applied to the transmission and the receiving, giving the highest quality of image.

The simple model for the STA ultrasound imaging is given in Fig. 1. In transmission only a single element is used. It creates a cylindrical wave (in the elevation plane the shape of the wavefront is determined by the height of the transducer) which covers the whole region of interest. The received echo comes from all imaging directions, and the received signals can be used to create a whole image – in other words all of the scan lines can be beamformed in parallel. The created image has low resolution because there is no focusing in transmit, and therefore in the rest of this report it is called a low-resolution image (LRI). After the first LRI, is acquired another element transmits and a second LRI is created. After all of the transducer elements have transmitted, the LRIs are summed and a high-resolution image is created.

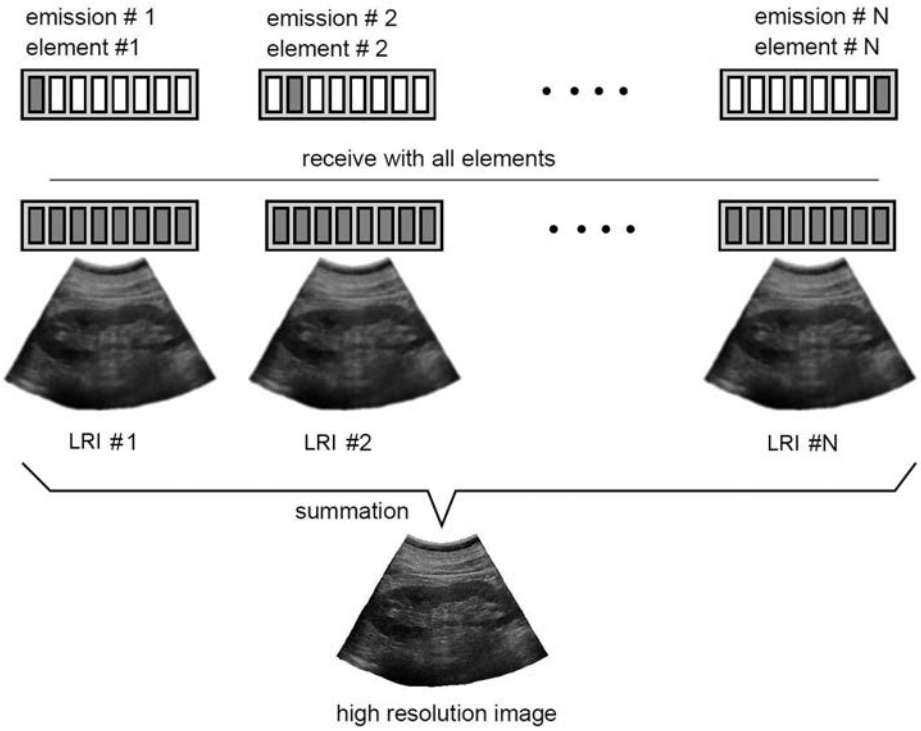

Fig. 1. LRIs combined to produce a high resolution image (after Nikolov, 2001).

In the SA ultrasound imaging methods for each point in the resulting image every combination of transmit-receive pairs contributes according to the round-trip propagation time only. The angular dependence is not taken into account in the applied point-like source model. But when the width of the array element

is comparable to the wavelength corresponding to the nominal frequency of the emitted signal, the point-like source model becomes inaccurate. Here, a STA imaging algorithm, which accounts for the element directivity function and its influence is applied (Tasinkevych *et al.*, 2012).

The underlying idea can be illustrated on the following example, shown in Fig. 2. Here, it is assumed, that the same element transmits and receives signal. Two scatterers located at the points with polar coordinates (r_i, θ_i), $i = 1, 2$ such that $r_{1m} = r_{2m}$ would contribute to the corresponding echo signal $y_{m,m}(t)$ simultaneously, since the round-trip propagation time $2r_{im}/c$, $i = 1, 2$ is the same. Apparently, the contribution from the scatterer at the point (r_1, θ_1) would be dominant, since the observation angle θ_{1m} coincides with the direction of maximum radiation for the m-th element, whereas its transmit-receive efficiency at the angle θ_{2m} is much smaller for the case of the scatterer at the point (r_2, θ_2). Thereby, evaluating the value of $A(r_2, \theta_2)$, the partial contribution of the echo $y_{m,m}(t)$, in addition to the correct signal from the obstacle located at (r_2, θ_2) (being small due to the large observation angle θ_{2m}), would also introduce the erroneous signal from the scatterer located at (r_1, θ_1). The later signal is larger due to the small observation angle θ_{1m}. The larger observation angles appear in the imaging region close to the array aperture. Therefore, the most appreciable deviation from the point-like source model of the array element will occur there. A solution to the problem, which accounts for the observation angle in accordance with the array element directivity function, is proposed. Assume, that the dependence of the transmit-receive efficiency of a single array element on the observation angle is known and is denoted by $f(\theta_m)$, where θ_m is measured from the line parallel to z-axis and passing through the m-th element center. Thus, in

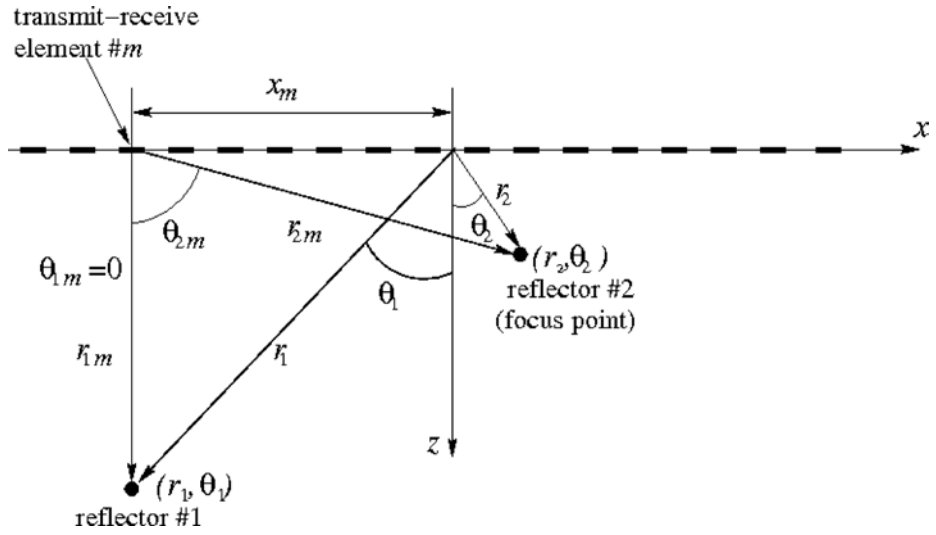

Fig. 2. Influence of the scatterer located at the point (r_1, θ_1) on the value of resulting signal $A(r_2, \theta_2)$ for imaging point (r_2, θ_2).

order to suppress the erroneous influence from the scatterer located at (r_1, θ_1) on the value of the resulting signal $A(r_2, \theta_2)$, the partial contribution of the echo $y_{m,m}(t)$ is weighted by the corresponding value of $f(\theta_{2m})$. This corresponds to the superposed signal correction in accordance with respective contributions of individual scatterers located at the points (r_1, θ_1) and (r_2, θ_2).

The above considerations lead to the following modification of the synthetic focusing imaging algorithm

$$A(r,\theta) = \sum_{m=1}^{N} \sum_{n=1}^{N} f(\theta_m) f(\theta_n) y_{m,n} \left(\frac{2r}{c} - \tau_{m,n} \right), \tag{1}$$

where $\theta_i(r,\theta)$, $i = m, n$ are the corresponding observation angles for the transmit-receive pair. The modification of the STA thus is expressed by a weighted summation of properly delayed RF signals (as in the case of conventional STA). The corresponding weights $f(\theta_m)$, $f(\theta_n)$ in the transmit and receive modes are calculated by means of the single element directivity function. Note, that the angles depend on the spatial location of the imaging point (r, θ). The directivity function $f(\theta)$ can be calculated in the far-field approximation for a single element of the array transducer in analogous manner as in (Selfridge *et al.*, 1980)

$$f(\theta) = \frac{\sin(\pi d/\lambda \sin\theta)}{\pi d/\lambda \sin\theta} \cos\theta, \tag{2}$$

where d is the element width, and λ is the wavelength.

3. Golay complementary sequences

Among the different excitation sequences proposed in ultrasonography, Golay codes evoke more and more interest in comparison with other signals. The reason of that lies in the fact that Golay codes, like no other signals, suppress to zero the amplitude of side-lobes. This type of complementary sequences has been introduced by Golay in the sixties (Golay, 1961). In the seventies the Golay complementary codes were implemented using interdigital transducers accounting for the Doppler effect in surface acoustic waves (SAW) devices (Danicki, 1974). The pairs of Golay codes belong to a bigger family of signals, which consist of two binary sequences of the same length n, whose auto-correlation functions have the side-lobes equal in magnitude but opposite in sign. The sum of these auto-correlation functions gives a single auto-correlation function with the peak of $2n$ and zero elsewhere (Trots *et al.*, 2004).

Figure 3 shows the pair of complementary Golay sequences, their autocorrelations, and the zero side-lobes sum of their autocorrelations.

As can be seen from the Fig. 3, the key to side-lobes canceling property of Golay code pairs is that the range side-lobes of one are equal in amplitude and opposite in sign to the side-lobes of the other.

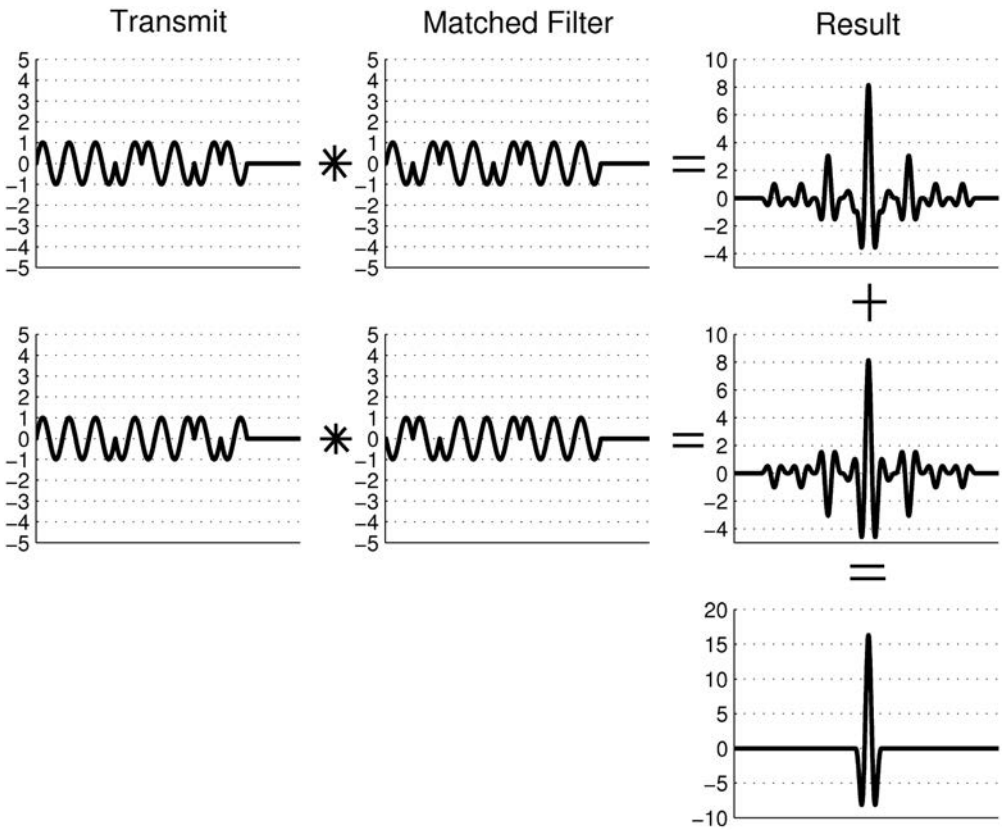

Fig. 3. Principle of side-lobes cancellation using pair of Golay complementary sequences of length 8 bits.

4. Computer simulation

Simulation is a fundamental way of testing methods. This is done to confirm or reject a hypothesis in a controlled environment. Since it is possible to control all parameters in a simulation, one can set up a simple model and then gradually transform it into something more similar to reality. When this is done one can continue with measurements and confirm or reject the simulations for a real setup, in vivo or on a phantom. All simulations in this work are carried out with a powerful software, *Field II*. The program is developed especially for investigating ultrasound fields, and gives the possibility to simulate and calculate ultrasound fields and defining one's own transducer. *Field II* runs under Matlab and the accuracy is very high since *Field II* is based on numerical analysis. The STA algorithm is used in the numerical examples presented in this paper.

The numerical results presented in Fig. 4 were performed for a 128-element linear transducer array with 0.3 mm pitch excited by one sine cycle burst pulse at

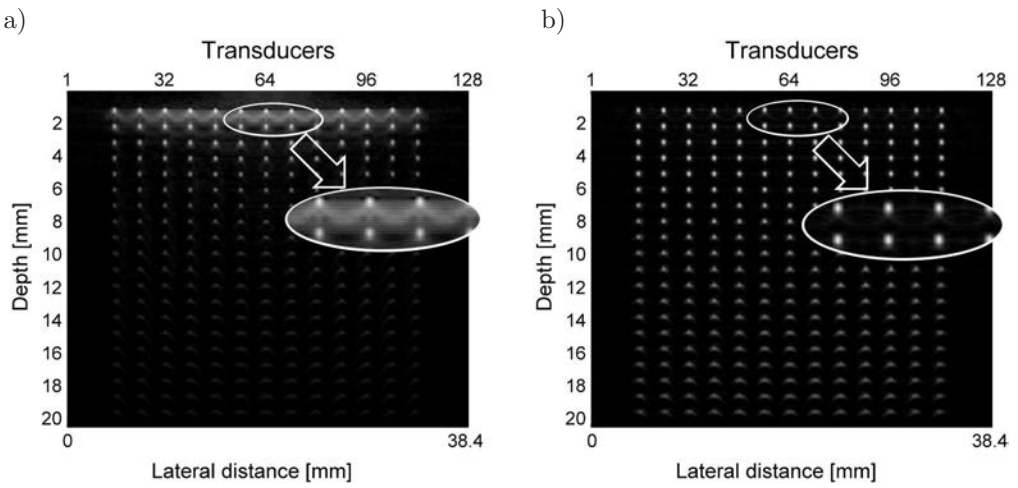

Fig. 4. Simulation of multi-point scatterers for 128-element linear array: a) not including directional diagram of element; b) including directional diagram of element. Marked area is magnified evidencing suppression of the "noise"-like spatial variations of the scattered signal from the reflectors positioned near the transducer surface.

a nominal frequency of 4 MHz. The element pitch is about λ, where λ corresponds to the nominal frequency of the burst pulse. The STA algorithm is employed. The transmit and receive elements combinations give a total of 128×128 possible RF A-lines. All these A-lines echo signals are sampled independently at a frequency of 40 MHz and stored in RAM.

The blurring of the scatterers placed near the aperture is significantly diminished in the case of introducing the directional diagram of element in synthetic focusing algorithm as compared to the algorithm without this correction

In Fig. 5 a computer simulation of multi-scatterers phantom when a 128-element linear transducer array was applied is shown. The one cycle as well as the pairs of complementary Golay sequences of the lengths 8 and 16 bits at nominal frequency 4 MHz were used. The phantom attenuation is equal to 0.5 dB/(MHz·cm). In the applied STA algorithm the element directivity correction scheme, discussed in (Tasinkevych *et al.*, 2012), was implemented to improve the image quality near transducer aperture.

The obtained 2D ultrasound images clearly demonstrate the advantage of using the Golay coded sequences. With the elongation of the coded sequences the acoustical energy increases yielding a higher SNR, that leads to an increase in the penetration depth while maintaining both axial and lateral resolution. The latter depends on transducer acoustic field and is discussed in (Nowicki *et al.*, 2007). The visualization depth when the one cycle was applied is equal to about 3 cm (Fig. 5a), while in case of applying 8-bits Golay codes this depth increases to 5 cm (Fig. 5b), and for longer 16-bits Golay codes this depth of visualization increases up to 7 cm (Fig. 5c).

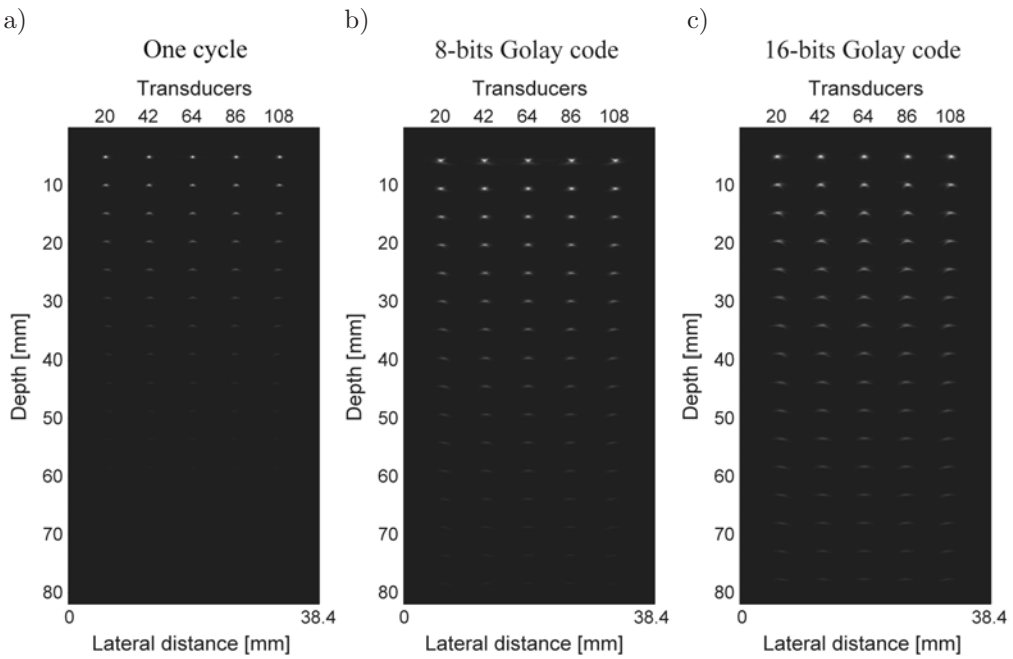

Fig. 5. Comparison of 2D ultrasound images obtained by computer simulation for 128-element linear array using: a) one cycle; b) 8-bits Golay sequences; c) 16-bits Golay sequences.

In order to compare the lateral resolution the cross-section of phantom at a depths of 10 mm and 30 mm is shown in Fig. 6. Note, the normalization is perform with respect to the maximum values of the corresponding cross-sections at different depth.

In Fig. 6 it can be seen that the lateral resolution at the different depths for all burst signals is the same. As anticipated, the lateral resolution illustrated in

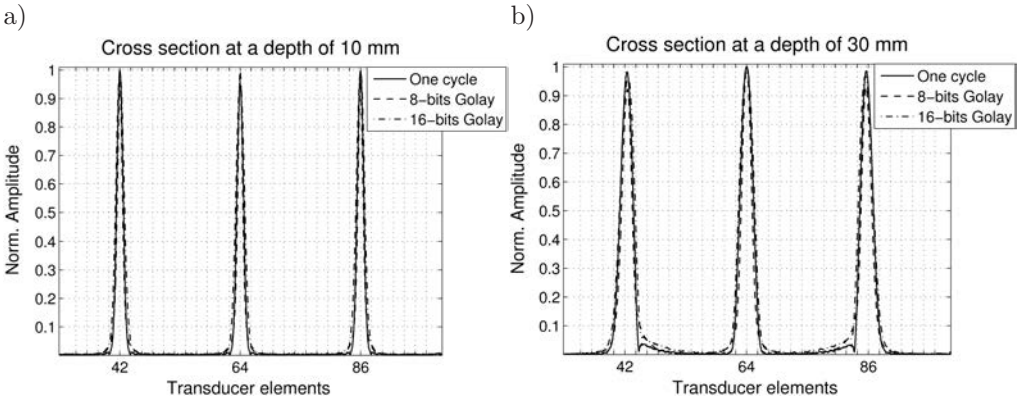

Fig. 6. Comparison of the lateral resolution at a depths of 10 mm (a) and 30 mm (b) when one cycle, 8 and 16-bits Golay sequences were applied.

Fig. 6 as a function of depth is almost unchanged for the Golay codes of different length (being the function of the system bandwidth it is independent of the code duration (Xu, Wang, 2003).

5. Ultrasound imaging system

A simplified block diagram of the experimental setup used in this work is shown in Fig. 7.

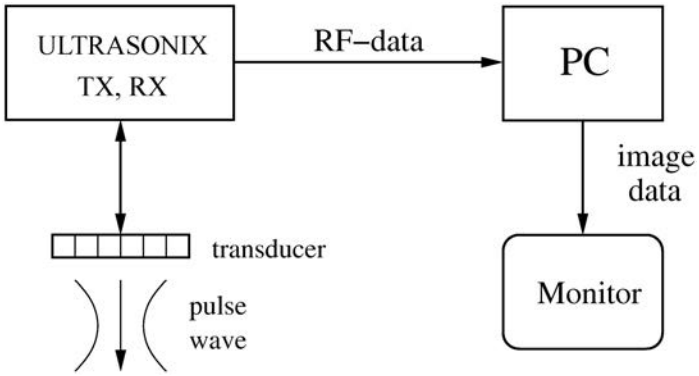

Fig. 7. Block diagram of the ultrasound imaging system.

It's main part is an Ultrasonix – SonixTOUCH Research System (Ultrasonix Medical Corporation, Canada) equipped with a 128-element linear transducer array. Ultrasonix enables a full control of transmission and reception parameters for all 128 elements of the transducer. Besides, a full access to raw RF data enables one to send it to the PC for further digital processing. Next, the processed data are displayed on the monitor. All post processing and display is done on PC using Matlab®. The processing creates 2D ultrasound image focused in every point.

In synthetic aperture imaging all scan lines (full image) are created in each and every firing, while in standard beamforming only a single line is created. The amount of raw RF data needed in the STA algorithm for an N-element ultrasound transducer for reconstruction of a single image is proportional to $D_{RF} \cdot M \cdot N$ and the number of delay-and-sum operations is $D_{RF} \cdot M \cdot N^2$, where D_{RF} is the number of samples in a single RF line. Thus, for the 128-element array, used in experiments, for 10 cm penetration ($D_{RF} = 5500$ at 40 MHz sampling frequency) storage requirements is $\approx 90 \cdot 10^6$ samples or ≈ 0.7 Gb of RAM (for 8 bytes per sample in Matlab® double precision format). And the total number of delay-and-sum operations in the STA image reconstruction algorithm is $\approx 11.5 \cdot 10^9$.

6. Experimental results and discussion

The 128-element linear transducer array excited by the 8 and 16-bits Golay coded sequences as well as a one cycle at nominal frequencies 4 MHz were used in the experiments. A single element in the transducer transmitting aperture was used to generate an ultrasound wave covering the full image region. All elements were used for both transmitting and receiving. The RF echo signals sampled independently at 40 MHz and processed by the STA algorithm. Experimental data were acquired by an Ultrasonix – SonixTOUCH Research System (Ultrasonix Medical Corporation, Canada).

The tissue mimicking phantom model 525 Danish Phantom Design with attenuation of background material 0.5 dB/(MHz·cm) was used. It consists of several nylon filaments twists 0.1 mm in diameter positioned every 1 cm axially. This phantom allows to examine the axial and lateral resolution at various depths in the ultrasound image.

The comparison of the 2D ultrasound images of the tissue phantom obtained for one cycle, 8-bits and 16-bits Golay complementary sequences is shown in Fig. 8. The peak pressure level of excitation signals at the transducer were set

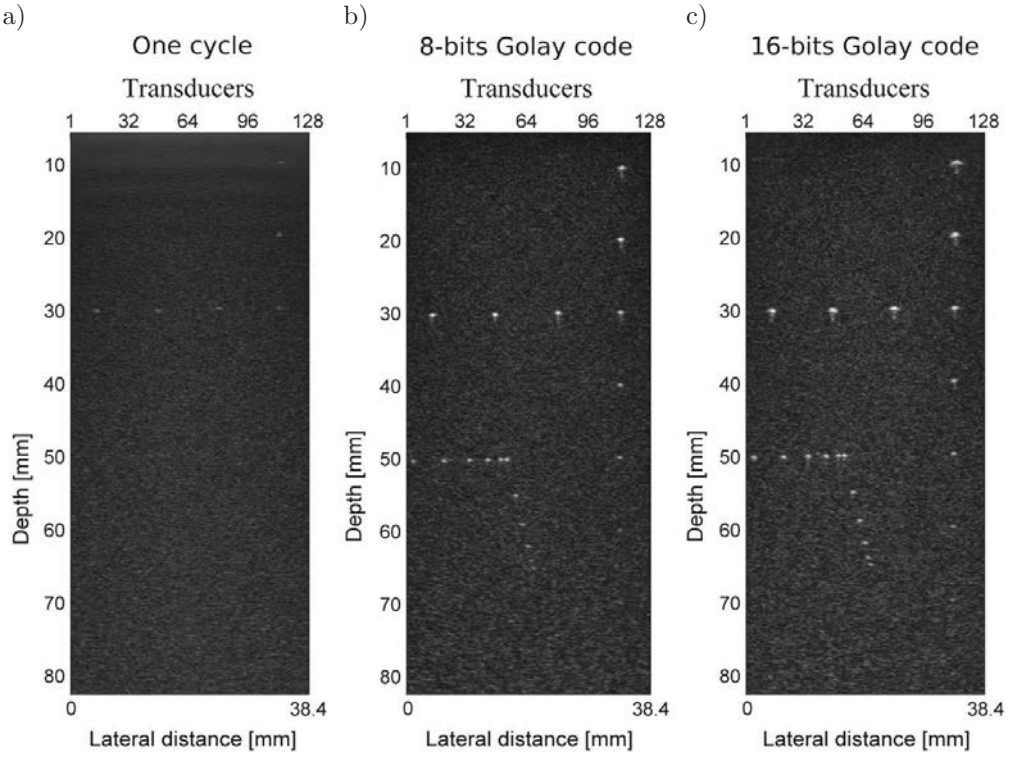

Fig. 8. 2D ultrasound images of tissue mimicking phantom using:
a) one cycle; b) 8-bits Golay code; c) 16-bits Golay code.

as low as possible to visually detect the echoes received using one cycle burst transmission slightly larger than the noise level. The same peak pressure has been used for the coded transmission.

The obtained 2D ultrasound images show an excellent performance of the coded excitation in terms of increasing penetration depth. In the case of one cycle the penetration depth is equal only to 3 cm (Fig. 8a). In the case of 8-bits Golay code the penetration depth increases up to 7 cm (Fig. 8b). With the elongation of the coded sequences to 16 bits the acoustical energy increases yielding higher SNR, that leads to an increase in the penetration depth up to 8 cm (Fig. 8c). Note that axial and lateral resolution is the same for the all burst signals.

In order to compare quantitatively the SNR gain the 112th line from 128 RF-lines of the 2D ultrasound images is shown in Fig. 9 and the SNR is calculated. For this purpose the noise level which appeared straight after the signal was chosen.

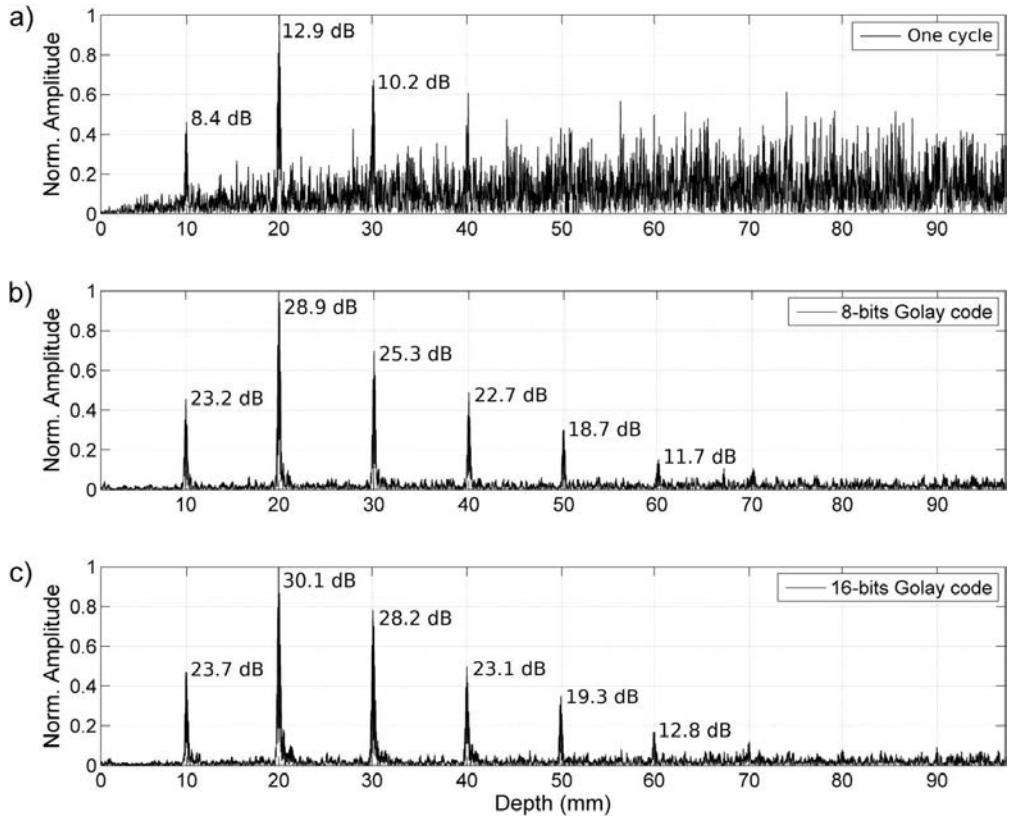

Fig. 9. The RF-lines of the tissue mimicking phantom using: a) one cycle; b) 8-bits Golay code; c) 16-bits Golay code.

Figure 9 shows that applying coded transmission in comparison to one cycle pulse allows to improve the SNR by about 15 dB. Elongating the coded transmission twice leads to the SNR increase by about 1.4 dB which is in agreement with the studies shown in (Trots *et al.*, 2004) where the final output is $2L$ times larger (L is the coded length) than the response to a single impulse; however, the noise increases by a factor of $\sqrt{2L}$($\sqrt{L}$ for each correlation and $\sqrt{2}$ for the addition). Therefore, an improvement in the SNR of $\sqrt{2L}$ is obtained in comparison with the single period burst transmission. More realistically, for transmit two sequences per observation time, the SNR improvement factor is $\sqrt{L}$. The SNR increase in its turn leads to improvement of the penetration depth and the contrast of the image.

7. Conclusion

Ultrasound imaging allows to visualize structures and organs in real-time, enabling an instantaneously evaluation of clinical situation. But real problems appear when the reconstruction of the deeply located organs is needed. For that reason, coded excitation can be used making examination procedure more precise and allowing visualization of the deeply located organs in 2D B-mode ultrasound imaging.

This work has addressed the problems in medical ultrasound imaging: improving of the penetration depth and gaining the SNR. To solve these problems, the complementary pairs of Golay coded sequences were used. The comparison of the 2D ultrasound images show that elongated coded sequences from 8-bits to 16-bits increase the penetration depth by about 2 cm. Applying of the coded transmission in the STA method in a standard ultrasound scanner could allow to increase the efficiency and quality of the ultrasound diagnostic. Moreover, the same coded sequences can also be used in conjunction with the multi-element synthetic transmit aperture (MSTA) method. This can further improve the penetration depth and image contrast, since several elements are used in transmit mode. It should be noted, however, that in the MSTA method in order to account for the multi-element transmit aperture directivity a proper modification of the algorithm is required, since the analytical Eq. (2) is no longer applicable. In this case the results of the full-wave analysis of radiation and scattering problems for a periodic (Tasinkevych, Danicki, 2010; 2011) or a finite (Tasinkevych, 2010) baffle system can be applied. The method is based on BIS-expansion (Blotekjaer *et al.*, 1973) of the wave-field Bloch component series into the finite series of Legendre polynomials, which was successfully applied to solving electrostatic problems in the theory of surface acoustic wave transducers (Danicki, Tasinkevych, 2006), in the theory of elastic wave scattering by periodic cracks (Danicki, 2002) and in the theory of EM scattering by periodic structures (Tasinkevych, 2008; 2009; 2011). Another advantage of the MSTA

algorithm as compared to the STA is the increase of the frame rate, which feature is of highest priority for implementation in the real time imaging applications. This is an ample topic for further research study.

Acknowledgments

This work was supported by the Polish Ministry of Science and Higher Education (Grant NN518382137).

References

1. Blotekjaer K., Ingebrigtsen K.A., Skeie H. (1973), *Methods for analyzing waves in structures consisting of metal strips on dispersive media*, IEEE Trans. Electron. Devices, **ED20**, 12, 1133–1138.
2. Danicki E.J. (1974), *Complementary code realization based on surface acoustic waves*, Bulletin of Military Technical Academy, XXIII (1), 53–56, 1974.
3. Danicki E.J. (2002), *Scattering by periodic cracks and theory of comb transducers*, Wave Motion, **35**, 4, 355–370.
4. Danicki E.J., Tasinkevych Y. (2006), *Nonstandard electrostatic problem for strips*, J. Electrostat., **64**, 6, 386–391.
5. Golay M.J.E. (1961), *Complementary series*, IRE Tran. Inf. Theory, **IT-7**, 82–87.
6. Hongxia Y. (1997), *Synthetic aperture methods for medical ultrasonic imaging*, Thesis.
7. Jensen J.A. (1996), *Field: A program for simulating ultrasound systems*, Paper presented at the 10th Nordic-Baltic Conference on Biomedical Imaging Published in Medical & Biological Engineering & Computing, **34**, Suppl. 1, Part 1, 351–353.
8. Klimonda Z., Lewandowski M., Nowicki A., Trots I. (2005), *Direct and post-compressed sound fields for different coded excitations – experimental results*, Archives of Acoustics, **30**, 4, 507–514.
9. Nikolov S.I. (2001), *Synthetic aperture tissue and flow ultrasound imaging*, PhD Thesis, Ørsted. DTU, Technical University of Denmark, 2800, Lyngby, Denmark.
10. Nowicki A., Klimonda Z., Lewandowski M., Litniewski J., Lewin P.A., Trots I. (2007), *Direct and post-compressed sound fields for different coded excitation*, Acoustical Imaging, **28**, 5, 399–407.
11. Nowicki A., Secomski W., Litniewski J., Trots I. (2003), *On the application of signal compression using Golay's codes sequences in ultrasound diagnostic*, Archives of Acoustics, **28**, 4, 313–324.
12. Selfridge A.R., Kino G.S., Khuri–Yakub B.T. (1980), *A theory for the radiation pattern of a narrow-strip acoustic transducer*, Appl. Phys. Lett., **37**, 1, 35–36.
13. Tasinkevych Y. (2008), *Scattering of H-polarized wave by a periodic array of thick-walled parallel plate waveguides*, IEEE Trans. Antennas Propagat., **56**, 10, 3333–3337.
14. Tasinkevych Y. (2009), *EM scattering by the parallel plate waveguide array with thick walls for oblique incidence*, J. Electromagn. Waves Appl., **23**, 11-12, 1611–1621.

15. Tasinkevych Y. (2010), *Wave generation by a finite baffle array in applications to beam-forming analysis*, Archives of Acoustics, **35**, 4, 677–686.

16. Tasinkevych Y. (2011), *Electromagnetic Scattering by Periodic Grating of Pec Bars*, J. Electromagn. Waves Appl., **25**, 5-6, 641–650.

17. Tasinkevych Y., Danicki E. (2010), *Full-wave analysis of periodic baffle system in beam-forming applications,* Archives of Acoustics, **35**, 4, 661–675.

18. Tasinkevych Y., Danicki E.J. (2011), *Wave generation and scattering by periodic baffle system in application to beam-forming analysis*, Wave Motion, **48**, 2, 130–145.

19. Tasinkevych Y., Trots I., Nowicki A., Lewin P.A. (2012), *Modified synthetic transmit aperture algorithm for ultrasound imaging*, Ultrasonics, **52**, 4, 333–342.

20. Trahey G.E., Nock L.F. (1992), *Synthetic receive aperture imaging with phase correction for motion and for tissue ihomogeneities – Part I: Basic principles*, IEEE Trans. Ultrason. Ferroelec. Freq. Contr., **39**, 4, 489–495.

21. Trots I., Nowicki A., Lewandowski M. (2009), *Synthetic transmit aperture in ultrasound imaging*, Archives of Acoustics, **34**, 4, 685–695.

22. Trots I., Nowicki A., Lewandowski M., Tasinkevych Y. (2010), *Multi-element synthetic transmit aperture in medical ultrasound imaging*, Archives of Acoustics, **35**, 4, 687–699.

23. Trots I., Nowicki A., Secomski W., Litniewski J. (2004), *Golay sequences – side-lobe canceling codes for ultrasonography*, Archives of Acoustics, **29**, 1, 87–97.

24. Xu M., Wang L.V. (2003), *Analytic explanation of spatial resolution related to bandwidth and detector aperture size in thermoacoustic or photoacoustic reconstruction*, Phys. Rev. E, **67**, 5, 1–15.